Off-center rattling and cage vibration of the carrier-tuned type-I clathrate $Ba_8Ga_{16}Ge_{30}$ studied by Raman scattering

Y. Takasu,[1] T. Hasegawa,[2] N. Ogita,[2] M. Udagawa,[2,3] M. A. Avila,[4] K. Suekuni,[4] and T. Takabatake[4,3]
[1]*Department of Physics, St. Marianna University School of Medicine, Kawasaki, Kanagawa 216-8511, Japan*
[2]*Graduate School of Integrated Arts and Sciences, Hiroshima University, Higashi-Hiroshima, Hiroshima 739-8521, Japan*
[3]*Institute for Advanced Material Research, Hiroshima University, Higashi-Hiroshima, Hiroshima 739-8530, Japan*
[4]*Graduate School of Advanced Sciences of Matter, Hiroshima University, Higashi-Hiroshima, Hiroshima 739-8530, Japan*
(Received 1 April 2010; revised manuscript received 7 September 2010; published 5 October 2010)

To reveal dynamical property of a guest ion in type-I clathrate compound, *n*- and *p*-type clathrates $Ba_8Ga_{16}Ge_{30}$ have been investigated by Raman scattering. It is found that the guest ion in a 6d-site cage (6d-cage) rotationally moves for both *n*- and *p*-type since the additional guest mode E_g(A) has been observed regardless of its carrier. The potential-energy difference between [100] and [110] directions in the 6d-cage is proportional to the off-center distance of the guest-ion position from the cage center and this off-center distance for *p*-type is much larger than that for *n*-type $Ba_8Ga_{16}Ge_{30}$. In addition, the Raman intensity of the cage vibration at a 6c site for *p*-type is weaker than that for *n*-type. Thus, the amplitude of the vibration at the 6c site becomes small for *p*-type, and this small amplitude induces a large movable space for the guest ion, i.e., this vibrational amplitude of the 6c-site atom works as the barrier for the off-center position. For both systems, the guest ion in the 6d-cage shows an anharmonic vibration, judging from the anomalous energy decrease in the guest ion with decreasing temperature. The energy difference between T_{2g} and T_{1u} [T. Mori *et al.*, Phys. Rev. B **79**, 212301 (2009)] of the guest mode clearly supports the theoretical prediction of an interacting dipoles picture that explains the glasslike properties of the off-centered clathrate. It is concluded that the off-center rattling plays an important role to suppress a lattice thermal conductivity.

DOI: 10.1103/PhysRevB.82.134302 PACS number(s): 63.20.−e, 63.50.−x, 78.30.−j

I. INTRODUCTION

Type-I clathrate compound is one of the promising candidates as a high performance thermoelectric material. It has been suggested that the rattling mode, due to the guest-ion motions in the host cage, plays a key factor to improve a thermoelectric performance since this mode is considered to suppress the lattice thermal conductivity [κ_L] by a scattering of heat-carrying acoustic phonons.[1–6] The suppression of κ_L is the essential factor to achieve high performance because the thermoelectric figure of merit inversely depends on the thermal conductivity.

Recently, a theoretical study suggests that not the mere rattling but the off-center rattling is crucial to suppress κ_L for the type-I clathrate.[7] According to the previous studies,[8–10] the off-center rattling is derived from the guest-to-cage size mismatch, where the size of the guest ion is smaller enough than the free space of the guest ion in the cage. For type-I clathrates $A_8Ga_{16}Ge_{30}$ (A=Eu, Sr, and Ba) with negative carrier, the guest positions in the cage have been investigated by the neutron diffraction[11–13] and by extended x-ray-absorption fine structure.[14] These experimental results have clarified that the guest position at a 2a-site cage is the on-center while that at the 6d-site cage (6d-cage) is the off-center for A=Eu and Sr, and is the almost center for A=Ba. The neutron-diffraction experiments have indicated that the guest ion at the 6d site moves in a plane perpendicular to a fourfold axis of the 6d-cage, and the off-center positions are not on the same plane.[11–13] The crystal structural analysis[12] and the first-principles calculations[15] have suggested that the off-center positions lie at 24k sites, which are the middle positions of the line between the 6d site and the 6c one as shown in Fig. 1(a).

These experimental and theoretical results suggest that not only the behavior of the guest ion in the 6d-cage but also the cage-atom motions for the 6c site is very important to understand the microscopical properties of the off-center rattling. In our previous Raman scattering study using single crystals of $A_8Ga_{16}Ge_{30}$, the lowest-energy phonon in two different symmetries has been assigned to the rotational guest motion based on the result of the first-principles calculations. The energy difference between two guest modes is about 4 cm^{-1} for A=Eu and Sr but is very small for A=Ba.[16]

The carrier-controlled single crystal of $Ba_8Ga_{16}Ge_{30}$ has been synthesized.[17] Instead of the similar crystalline structure between *n*-type $Ba_8Ga_{16}Ge_{30}$ (*n*-Ba) and *p*-type one (*p*-Ba), the κ_L for *p*-Ba shows the glasslike temperature dependence with a plateau around 10–30 K (Refs. 17 and 18) while that for *n*-Ba has a normal crystalline peak around 10 K.[11,17,18] Recently, it has been reported that the Ba ion in the 6d-cage for *n*-Ba as well as for *p*-Ba is displaced clearly to the off-center position.[19,20] Christensen *et al.* have reported that the dynamical behavior of the guest ion shows the subtle difference.[19] They have suggested that the main difference between *n*- and *p*-Ba is found in the cage structure and that the difference of the occupancy of Ga to Ge would be a key factor for the behavior of the κ_L against temperature. Tang *et al.* have also suggested by their x-ray photoelectron spectroscopy studies that there are two positions of the guest ion at the 6d site.[20] In addition, they have pointed out that the off-center mode has a strong relationship with the Ga position in the cage.

In this paper, we mainly discuss three subjects for both *n*- and *p*-Ba, based on the results of the polarization dependence and the temperature dependence of the Raman spectra. One

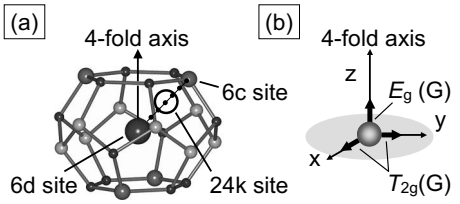

FIG. 1. (a) The 6d-cage of type-I clathrate compound. The 24k site is located at the off-central position near the 6d site toward the 6c site. (b) Raman-active modes for the guest ion with the center position in the 6d-cage. See text in details.

is the difference of the dynamical behavior of the guest ion in the 6d-cage between *n*- and *p*-Ba. The second is the effect of the cage vibration on the guest motions, and we present the possible formation mechanism of the off-center rattling. The third is the temperature dependence of the Raman spectra and the guest energies. Finally, we present the importance of the off-center rattling, not the mere rattling, for the suppression of κ_L.

II. EXPERIMENTAL

Raman spectra were measured by a triple monochromator (JASCO NR-1800) with a liquid N_2-cooled charge coupled device (CCD) detector (Princeton Instruments Inc. LN/CCD-1100PB) in the temperature region between 2 K and room temperature. The excitation light was 514.5 nm wavelength Ar-ion laser with a power of 10 mW at the specimen. All measurements in this study were carried out using single crystals. Sample preparation was already reported in the papers.[16,18]

The symmetry of type-I clathrate compounds is $Pm\bar{3}n$. The Raman-active phonons are given by a group theoretical estimation as $3A_{1g}+7E_g+8T_{2g}$ for the cage, and E_g+T_{2g} for the guest at the 6d-cage under the assumption of the center position. Two estimated guest modes are shown in Fig. 1(b) while the guest motions at the 2a site are not Raman active. These phonons with each irreducible representation have been assigned by the polarization dependence. The polarization geometry is given by the notation (i,j), where i and j denote the polarization directions of the incident and scattered light, respectively. For example, phonon modes with A_{1g} and T_{2g} symmetry appear in (x,x) and (x,y) geometries, respectively, where x and y denote [100] and [010] axes. The phonon mode with E_g symmetry appears in both (x,x) and $(x+y,x-y)$ geometries.

The phonon energies were calculated for $Ba_8Ga_{16}Ge_{30}$ by the first-principles calculations under the assumption of the center position for the guest ion at the 6d-cage. The details of the calculations were reported in our previous paper.[16]

III. RESULTS AND DISCUSSION

A. Guest mode

Figure 2 shows the Raman spectra of *n*- and *p*-Ba at room temperature. Open and filled triangles indicate the Raman-active phonons obtained by the first-principles calculations

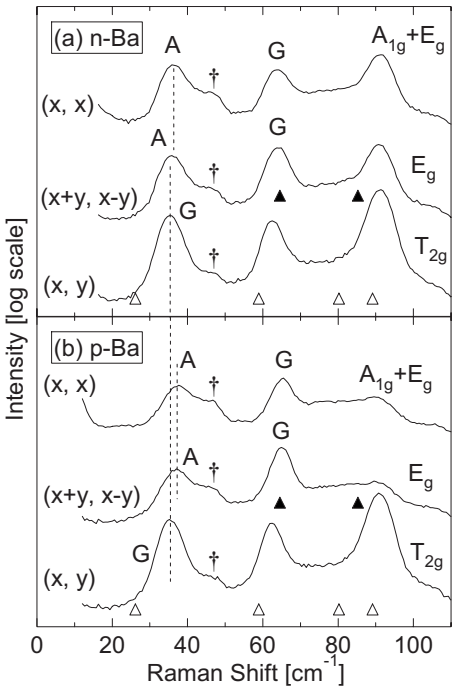

FIG. 2. Raman spectra of $Ba_8Ga_{16}Ge_{30}$ at room temperature. (a) *n*-type (*n*-Ba) and (b) *p*-type (*p*-Ba). Open and filled triangles indicate the Raman-active modes obtained by the first-principles calculations for $Ba_8Ga_{16}Ge_{30}$. The peaks marked by G and A indicate allowed guest mode and additional guest mode, respectively.

for $Ba_8Ga_{16}Ge_{30}$.[16] The phonon-mode assignment has been carried out referring to the results of the first-principles calculations. The allowed guest modes, i.e., E_g and T_{2g}, are marked by "G" in Fig. 2, where the intensity is depicted in logarithmic scale. For convenience, these modes are named E_g(G) and T_{2g}(G), respectively. Furthermore, the additional guest mode marked by "A" has been observed in the $(x+y,x-y)$ polarization for both systems [hereinafter called E_g(A)]. This additional mode E_g(A) has been also observed for *n*-type $Eu_8Ga_{16}Ge_{30}$ (*n*-Eu) and *n*-type $Sr_8Ga_{16}Ge_{30}$ (*n*-Sr), and has been assigned to the tangential movement along [110] direction in the basal plane.[16,21] The unidentified structure has been observed on the high-energy side of both E_g(A) and T_{2g}(G) marked by daggers. This structure has been also confirmed in the (x,x) geometry. The detail of this structure is discussed in Sec. III C. However, since the guest energies have been determined by the mode analysis including several Lorentz functions with the unidentified structure, the effect of this structure to the guest modes can be ignored.

Here, the detailed group theoretical consideration for E_g(A) is presented since its existence is very important for the rotation of the guest ion at the off-center position, especially for *n*-Ba. The center position is not the case since $E_g(A)$ is not Raman active as shown in Fig. 1(b). Next case is the off-center position with the displacement along [100] without rotational motion. In this case, the site symmetry of the guest becomes *m*, 2, or 1, as the results, many components of the Raman tensors for the guest vibrations have nonzero values. This concludes that all vibrations should be found in all polarization geometries, i.e., (x,x), $(x+y,x-y)$, and (x,y), without the polarization selection rule. However,

in the actual Raman spectra for *n*-Eu and *n*-Sr, clear polarization dependence and different energies have been observed for three guest modes.[16] The last case is the rotational guest motion in the basal plane. In this case, the cage symmetry is $\bar{4}2m$ with the fourfold axis parallel to $\bar{z}$. The displacements for the guest motion in the basal plane are classified as follows. One is the radial displacement with the total symmetric A_1 representation. The second is the rotational displacement around the cage center. The eigenfunctions or base vectors of this rotation correspond to $\bar{x}\bar{y}$ and $\bar{x}^2-\bar{y}^2$, which belong to the representations of B_1 and B_2, respectively, in $\bar{4}2m$. If the guest ion rotates in the isotropic potential with the rotational symmetry around $\bar{z}$, two representations B_1 and B_2 degenerate, i.e., there is no energy difference between them. However, the existence of the $\bar{4}$ symmetry breaks this degeneracy and the excitation energy becomes different between them. The Raman tensors of A_1, B_1, and B_2 in $\bar{4}2m$ are depicted below,

$$R^{A_1} = \begin{pmatrix} a & 0 & 0 \\ 0 & a & 0 \\ 0 & 0 & c \end{pmatrix},$$

$$R^{B_1} = \begin{pmatrix} b & 0 & 0 \\ 0 & -b & 0 \\ 0 & 0 & 0 \end{pmatrix}, \quad R^{B_2} = \begin{pmatrix} 0 & e & 0 \\ e & 0 & 0 \\ 0 & 0 & 0 \end{pmatrix}. \tag{1}$$

Thus, the radial vibration appear in (x,x), and the rotational excitations can be observed in (x,x) and $(x+y,x-y)$ for B_1 and in (x,y) for B_2. Since the crystal symmetry of the clathrates is $Pm\bar{3}n$, the compatibility relation between $\bar{4}2m$ and $Pm\bar{3}n$ concludes that the radial vibration A_1 becomes A_{1g}, the rotational excitation B_1 is E_g, and the rotational excitation B_2 is T_{2g}. It should be noted that three excitations have different representation with the *different* energy in $Pm\bar{3}n$. The vibration along $\bar{z}$ is not changed and can be observed in the E_g spectrum.

For both *n*- and *p*-Ba, the guest ion in 6d-cage moves rotationally around the cage center regardless of its carrier since the additional mode E_g(A) is clearly observed. This is the experimental evidence of the off-center position and the rotational motion of the guest ion. The off-centered rotational property of the guest ion would be attributed to the anharmonic potential of the 6d-cage. As discussed later, the 6d-cage of both *n*- and *p*-Ba forms the anharmonic potential, which is clarified by the anomalous energy decrease in the guest modes on cooling. Once, in our previous report,[16] we could not discuss the details of the rotational guest motion for *n*-Ba since there were not any experimental reports of its off-center position at that time.

As mentioned above, T_{2g}(G) and E_g(A) modes correspond to the tangential motions along [100] and [110] directions in the basal plane. If the guest ion can move almost freely in the basal plane, i.e., the potential shows the isotropic feature, the energy of T_{2g}(G) would be almost the same to that of E_g(A). For *n*-Ba, the energy of T_{2g}(G) is very close to that of E_g(A). This means the small anisotropy between the [100] and [110] directions in the 6d-cage. For *p*-Ba, however, the energy of T_{2g}(G) is clearly lower than that of E_g(A) as shown in Fig. 2. The *p*-Ba case is quite similar to the *n*-Eu case where the off-center distance is the largest among the GaGe-cage type-I clathrates. Thus, the potential at the 6d-cage for *p*-Ba shows the anisotropic feature between the [100] and [110] directions. The result of $T_{2g} < E_g$ for the guest energies indicates that the stable positions lie toward the [100] directions rather than toward [110]. This is consistent with the previous results.[11,19]

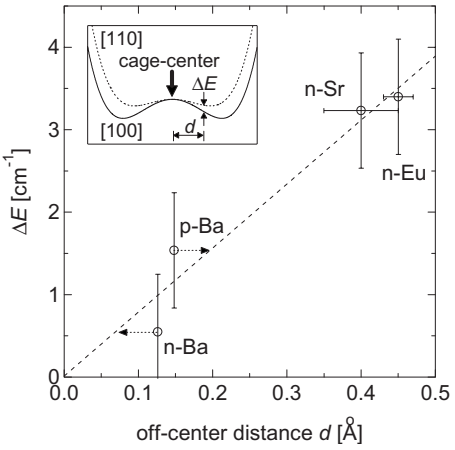

FIG. 3. The relationship between the off-center distance (Refs. 14 and 19) and ΔE. ΔE is the energy difference between two guest modes.

Further, if the potential at the 6d-cage is the four-well type as shown in the inset of Fig. 3, where the potential minima toward the [100] directions is lower than those toward [110], the energy difference between T_{2g}(G) and E_g(A), i.e., the energy difference between [100] and [110] directions probably correlates with the off-center distance. To clarify the relationship between the off-center distance (d) and the energy difference between T_{2g}(G) and E_g(A) (ΔE), ΔE is plotted as a function of d in Fig. 3. The d values for *n*-Eu and *n*-Sr are referred to Ref. 14, and for *n*- and *p*-Ba to Ref. 19. The ΔE values for *n*-Sr and *n*-Eu are referred to our previous study,[16] and those for *n*- and *p*-Ba are obtained from the temperature dependence of the guest energy, as discussed later. The dashed line is determined by the least-squares fitting using data of *n*-Eu, *n*-Sr, and the original point. The reason why we used the original point is that the limit of $d \rightarrow 0$ corresponds to that of $\Delta E \rightarrow 0$ as depicted in the inset of Fig. 3. Additionally, the data points of *n*- and *p*-Ba are close to the dashed line. Thus, it is plausible that the inset of Fig. 3 depicts the relationship between d and ΔE. According to the dashed line, we can estimate the d value for the *n*- and *p*-Ba. The plot of ΔE just on this dashed line gives us to extrapolate the following d values; 0.20 Å for *p*-Ba and 0.07 Å for *n*-Ba. This carrier dependence of d would strongly correlate with the cage dynamics as discussed in the next section.

Here, it is noteworthy to mention the relationship of the guest motions between the nearest-neighboring 6d-cages. The guest motion in 6d-cage for *p*-Ba forms an electric dipole due to the large off-center distance. Recently, Mori *et al.*

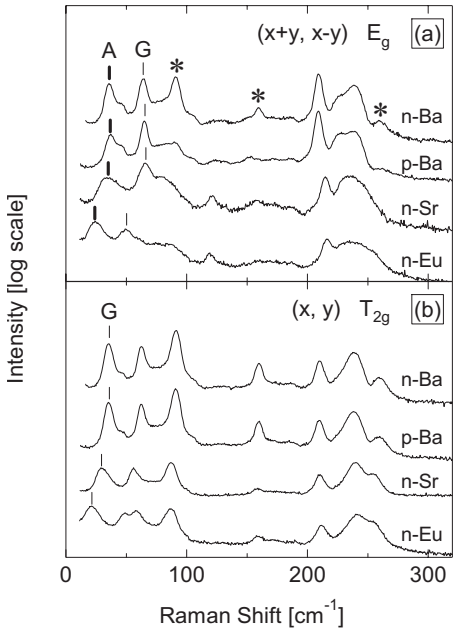

FIG. 4. Polarization dependence of the Raman spectra for *n*-type $Ba_8Ga_{16}Ge_{30}$ (*n*-Ba), *p*-type $Ba_8Ga_{16}Ge_{30}$ (*p*-Ba), *n*-type $Sr_8Ga_{16}Ge_{30}$ (*n*-Sr), and *n*-type $Eu_8Ga_{16}Ge_{30}$ (*n*-Eu) at room temperature. The peaks marked by G and A indicate allowed and additional guest mode, respectively. (a) is the spectra of $(x+y,x-y)$ geometry and (b) is those of (x,y) one. The marked modes by asterisks are described in the text.

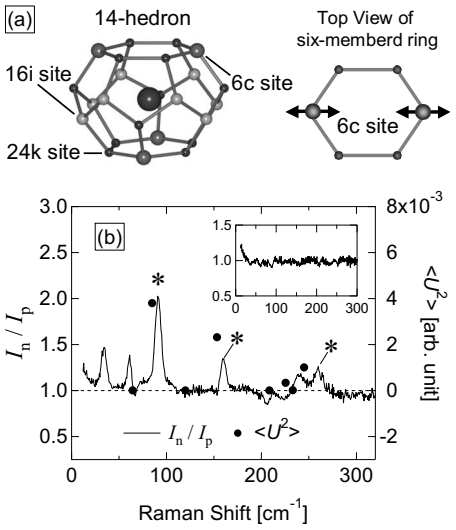

FIG. 5. (a) The site symmetry of 6d-cage atom (left) and 6c-site vibration with E_g symmetry (right). (b) Spectral ratio of the E_g spectrum for *n*-Ba to that for *p*-Ba, and mean-square atomic displacements $\langle U^2 \rangle$ at the 6c site for each mode are also shown by closed circles. Inset is the spectral ratio of the T_{2g} mode between *n*- and *p*-Ba.

have reported the energy of the rattling phonon for *p*-Ba using the terahertz time-domain spectroscopy (THz-TDS).[22] The THz-TDS can observe the T_{1u} mode, where the direction of the guest movement in one 6d-cage is the same in the nearest-neighbor 6d-cage, i.e., the direction of the dipole moment is the same between them. On the other hand, since T_{2g}(G) obtained by the Raman scattering is even parity, the guest motion is opposite between nearest-neighboring 6d-cages. Such dipole field effects on the energy of T_{1u} and T_{2g} since the T_{1u} against the dipole field direction and T_{2g} parallel to the dipole field. The energy of T_{1u} of the guest ion is larger by about 6 cm^{-1} than that of T_{2g}. This result is the experimental evidence for the existence of the interacting dipoles in the 6d-cages as predicted by the theory.[7]

B. Cage mode

Figure 4 shows the polarization dependence of the Raman spectra for *n*-Ba, *p*-Ba, *n*-Sr, and *n*-Eu at room temperature. At first, we discuss about the spectral difference between *n*- and *p*-Ba. Marked difference is clearly observed in the spectrum of $(x+y,x-y)$ geometry, where marked peaks are depicted by asterisks in the Fig. 4(a) and are the vibration of 6d-cage atom but the remarkable difference is not found in that of (x,y) geometry. Further, for the spectrum of (x,x) geometry, in which the $A_{1g}+E_g$ modes are observed, the spectral difference between *n*- and *p*-Ba are attributed to the asterisk modes in E_g mode, not due to A_{1g} as well as T_{2g} one.

To identify the site showing the spectral difference marked by the asterisks, we employ the result of the first-principles calculations. The first-principles calculations indicate that the marked modes by the asterisks correspond to the atomic vibrations at the 6c site with the large amplitude as shown in Fig. 5(a). Nonmarked modes in E_g spectrum and all T_{2g} modes are the atomic vibrations at the 24k and 16i sites, and those with zero or very small amplitude at the 6c site. Thus, the atomic vibrations of the cage are not affected by the carrier type except for the 6c vibration with the large amplitude. The vibrational amplitude at 6c site is crucial factor for the guest motions in the 6d-cage since the off-center positions are displaced toward the 6c site.

The ratio of $(x+y,x-y)$ spectrum between *n*- and *p*-Ba (I_n/I_p) is shown in Fig. 5(b). The clear carrier dependence is found for three characteristic peaks marked by asterisks in Fig. 5(b), which is the same marked modes in Fig. 4(a). The other peaks and dips are due to the slight energy shift for each mode. The mean-square atomic displacements $\langle U^2 \rangle$ at the 6c site for the E_g modes obtained by the first-principles calculations are depicted by the closed circles in Fig. 5(b). For the marked modes in Fig. 5(b), the sequence of the intensity almost coincides with that of the $\langle U^2 \rangle$ among three modes. Thus, the spectral difference of the E_g mode between *n*- and *p*-Ba corresponds to the difference of the vibrational amplitude of the cage atom at the 6c site as shown in Fig. 5(a). This indicates that the guest motions toward [100] direction for *p*-Ba differ from those for *n*-Ba. As shown in Figs. 4(a) and 5(b), the vibrational amplitude at the 6c site for *p*-Ba is smaller than that for *n*-Ba, yielding to enlarge the movable space for the guest ion in the 6d-cage. As the results, the guest ion for *p*-Ba can move with large off-center distance. On the other hand, for *n*-Ba, the large vibrational amplitude at the 6c-site atoms interrupts to displace the guest ion from the cage center. The (x,y) spectrum shows no carrier dependence as shown in the inset in Fig. 5(b), where the intensity ratio between *n*- and *p*-Ba is almost 1. It is note-

worthy that no spectral difference between *n*- and *p*-type in $Ba_8Ga_{16}Sn_{30}$ has been reported for every polarization geometry since their off-center distance is the same.[23]

Next, we discuss the spectral features among *p*-Ba, *n*-Sr, and *n*-Eu. The spectral feature for *p*-Ba is similar to that for *n*-Sr and *n*-Eu, especially the marked modes by asterisks. This means that the vibrational amplitude at the 6c site is also small for *n*-Sr and *n*-Eu whose off-center distance is considerably larger than the *p*-Ba case. Thus, the small vibrational amplitude at the 6c site enhances the large off-center distance in the 6d-cage, and this cage property is very important for GaGe-cage clathrates. Further, as shown in Fig. 4(b), the energy and the intensity of the cage modes around 100 and 150 cm^{-1} lowers in sequence of *p*-Ba, *n*-Sr, and *n*-Eu. This clearly shows that the considerably large off-center distance as *n*-Sr and *n*-Eu affects not only E_g cage modes but also T_{2g} cage modes. Therefore, the off-center rattling with the large displacement effectively lowers the cage stability, and this is the important property to suppress the κ_L.

The ratio of Ga to Ge is important factor to tune the carrier type in the Ba clathrate, where Ga/Ge for *n*-Ba is higher than that for *p*-Ba,[19] and Ga atom preferentially occupies the 6c site. According to Carrillo-Cabrera *et al.*, the Ge rich sample (*p*-Ba) contains vacancies at the 6c site.[24] The vacancies at the 6c site directly make the large movable space for the guest ion toward [100] direction. So, it seems that Ge-rich sample effectively increases the movable space for the guest ion. Unfortunately, at this stage, we cannot answer microscopically why the vibrational amplitude at the 6c site is large for *n*-Ba and small for *p*-Ba. However, we can claim that the electronic interaction between the guest ion and the 6c atom is very important to understand the correlation between the vibrational amplitude at the 6c site and the off-center distance of the guest ion at the 6d-cage.

In our previous work,[16] we assigned E_g modes for *n*-Ba without 260 cm^{-1} mode. In this study, it is revealed that the mode at 260 cm^{-1} in the $(x+y,x-y)$ spectrum for *n*-Ba originates from the large vibrational amplitude at the 6c site. In the large off-center distance systems, the marked modes including 260 cm^{-1} mode in Fig. 4(a) are very important.

C. Temperature dependence

Figures 6 and 7 are the temperature dependence of the Raman spectra and the guest energies, respectively, for *n*- and *p*-Ba. Previously, we have reported that the peak shape of the guest modes changes drastically from single peak to quite broad one below ~50 K for *n*-Eu and at 2 K for *n*-Sr.[16] Such change is against to the ordinary case where the spectral shape becomes sharp at low temperature. This spectral change in the guest mode has been understood by the change in the vibrational state, where the contribution of the quantum tunneling to the thermal rattling becomes dominant at low temperature. In addition, the energy coincidence of T_{2g}(G) and E_g(A) for *n*-Eu and *n*-Sr also suggests that the guest motion changes from the thermal rattling to the mixed state of the thermal rattling and the quantum tunneling. However, for Ba cases, the spectral changes in the guest mode,

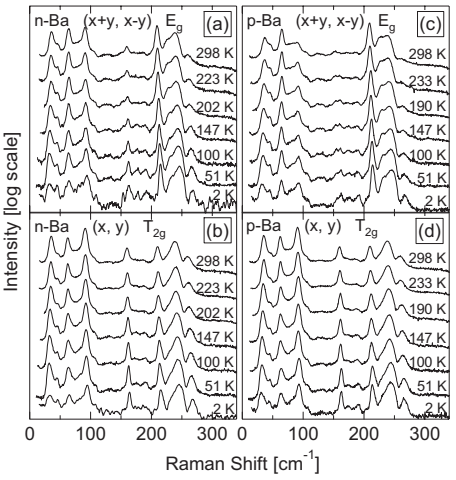

FIG. 6. Temperature dependence of Raman spectra of $Ba_8Ga_{16}Ge_{30}$. (a) and (b) *n*-type (*n*-Ba) and (c) and (d) *p*-type (*p*-Ba). (a) and (c) are for $(x+y,x-y)$ and (b) and (d) are for (x,y), respectively.

except for the decrease in its intensity, have not found at low temperature even for *p*-Ba as shown in Fig. 6, and the energy coincidence of T_{2g}(G) and E_g(A) has not been observed for both *n*- and *p*-Ba as shown in Fig. 7. Further, the very recent Raman-scattering study indicates that this energy coincidence has not been observed for $Ba_8Ga_{16}Sn_{30}$ at low temperature.[23] Thus, the thermal rattling is the dominant motion for the Ba ion not only in GaGe-cage but also in GaSn-cage even at low temperature. This is the typical character for the Ba ion.

As shown in Fig. 7, the guest energies anomalously decrease with decreasing temperature for both systems. The similar decrease has been also observed for *n*-Sr and *n*-Eu.[16] The origin of the anomaly can be explained by the large

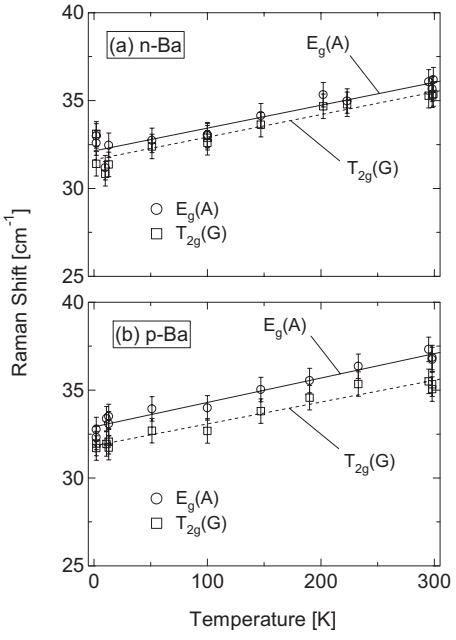

FIG. 7. Temperature dependence of the guest energies of $Ba_8Ga_{16}Ge_{30}$. (a) *n*-type (*n*-Ba) and (b) *p*-type (*p*-Ba).

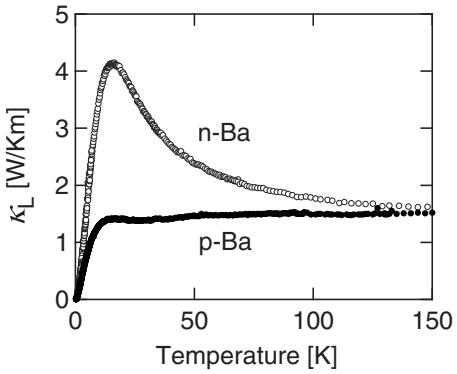

FIG. 8. Temperature dependence of the lattice thermal conductivity (κ_L) for *n*-Ba and *p*-Ba.

contribution of the fourth-order anharmonic potential at the 6d-cage. Thus, this anomaly is universal property for type-I clathrate compounds regardless of the carrier type. Recently, except for type-I clathrates,[16,21,22,25] the anomalous energy decrease has been observed in caged compounds of β-pyrochlore,[26] filled skutterudite,[27,28] and $La_3Pd_{20}Ge_6$,[29] and a layered compound of CaAlSi.[30] We note such energy decreases do not occur for the small cage.[27,29] Therefore, for the loosely bounded guest atom, the energy decrease on cooling is a universal phenomenon for the guest motion due to the fourth-order anharmonic potential.

Here, we note several spectral profiles. One is the unidentified structure observed on the high-energy side of the guest mode. This unidentified structure might be attributed to the A_{1g} mode, of which movement is radial direction at the off-center position, judging from its low energy. Such A_{1g} mode in *n*-Eu has been already reported in our previous paper.[16] However, the present mode in Ba case is different from the A_{1g} mode in *n*-Eu in the following properties. The A_{1g} mode appears only in the (x,x) polarization in *n*-Eu but that appears in every polarization geometries. This is against the off-center rotational motion since its poor polarization property suggests that the guest ion is trapped at certain off-center position as describe in the symmetrical discussion. This reason is not clear at this stage but we point that the short time trapping might be occur in *n*- and *p*-Ba. Such mode has not been observed in $Ba_8Ga_{16}Sn_{30}$.[23] The next difference is the temperature dependence of their guest energy. The guest energy of the A_{1g} mode in *n*-Eu has decreased on heating[16] while that of the unidentified mode for Ba case has increased on heating. Thus, to assign the unidentified mode as A_{1g} in *n*- and *p*-Ba, it is necessary to clarify at higher temperature region whether its energy decreases with increasing temperature or not.

The second is the change in the spectral profile in 150–200 cm^{-1} region, where unknown additional structures, which are not obtained by the first-principles calculations, are found on cooling. We point out the deformation of the cage or the inhomogeneous distribution of Ga/Ge atoms as the observation of these structure.

Finally, we discuss $\kappa_L(T)$ based on the present results. Figure 8 shows the $\kappa_L(T)$ for *n*- and *p*-Ba. The $\kappa_L(T)$ for *n*-Ba has the normal crystalline peak around 10 K while that for *p*-Ba shows the glasslike behavior with the typical plateau. Recently, the theoretical study has suggested that the dipole-dipole interaction between guest ions is crucial role to glasslike properties in type-I clathrate.[7] Since the off-center distance for *p*-Ba is larger than that for *n*-Ba, the dipole-dipole interaction between 6d guests is much large in *p*-Ba, compared with the *n*-Ba case. Thus, it can be concluded that the large off-center distance is crucially important factor to the glasslike behavior of the $\kappa_L(T)$.

IV. CONCLUSION

We have clarified the dynamical motions of the Ba ion in the 6d-cage by the Raman-scattering experiments for both *n*-Ba and *p*-Ba. The additional mode is observed in the $(x+y,x-y)$ spectrum regardless of its carrier type. The guest ion in the 6d-cage for *n*-Ba as well as for *p*-Ba is not located at the cage center, and rotates around the cage center even for *n*-Ba. The energy difference between the additional guest mode E_g(A) and the allowed guest mode T_{2g}(G) is clearly found for *p*-Ba while that is very small for *n*-Ba. The clear correlation between this energy difference and the off-center distance has been confirmed. The relationship reveals that the off-center distance for *p*-Ba is about three times as large as that for *n*-Ba. The temperature dependence of the Raman spectra shows that the thermal rattling, not the quantum tunneling, is the dominant guest motion for *p*-Ba as well as for *n*-Ba, even at low temperature. The anomalous decrease in the guest energy on cooling indicates that the guest ion moves in the 6d-cage with the anharmonic potential for both systems. The spectral differences between *n*- and *p*-Ba in $(x+y,x-y)$ spectrum are assigned as the difference of the atomic motion at the 6c site on the cage, with the sake of the first-principles calculations results. These experimental and calculated results suggest that the origin of the off-center position rattling would be attributed to the weak vibrational amplitude at the 6c site. The large off-center distance effect on the cage atom has been clearly observed even for the T_{2g} spectrum. Such cage dynamics due to this large off-center distance is important for the suppression of the κ_L. The experimental results of Raman scattering and THz-TDS have supported the theoretical prediction of the interacting dipoles in the 6d-cage. We think the off-center rattling with larger displacement is important for the glasslike κ_L(T).

Finally, we note the usage for the term of the *rattling*. In this study and our previous studies,[16,21] the dynamical properties of the *off-center rattling* as well as the effect of the off-center rattling on the cage property have been clarified microscopically. At this stage, according to the Slack's definition,[31] we propose that the term of the *rattling* should be used only for the case, where the lattice thermal conductivity is suppressed.

ACKNOWLEDGMENTS

This work was supported by COE Research of Ministry of Education, Sports, Culture, Science and Technology (Grant No. 13CE2002), a Grant-in-Aid for Scientific Research

Priority Area "Skutterudite" (Grant No. 15072205), the Priority Area "Nanospace" (Grant No. 19051011), the Innovative Area "Heavy Electrons" (Grants No. 20102004 and No. 20102005), the Scientific Research (A) (Grant No. 18204032), the Young Scientists (B) (Grant No. 21740257), and the Scientific Research (C) (Grant No. 21540328). The low-temperature experiments have been supported by N-BARD and IAMR of Hiroshima University.

[1] A. Bentien, E. Nishibori, S. Paschen, and B. B. Iversen, Phys. Rev. B **71**, 144107 (2005).
[2] A. Bentien, M. Christensen, J. D. Bryan, A. Sanchez, S. Paschen, F. Steglich, G. D. Stucky, and B. B. Iversen, Phys. Rev. B **69**, 045107 (2004).
[3] S. Paschen, W. Carrillo-Cabrera, A. Bentien, V. H. Tran, M. Baenitz, Y. Grin, and F. Steglich, Phys. Rev. B **64**, 214404 (2001).
[4] C. W. Myles, J. Dong, O. F. Sankey, C. A. Kendziora, and G. S. Nolas, Phys. Rev. B **65**, 235208 (2002).
[5] G. S. Nolas and C. A. Kendziora, Phys. Rev. B **62**, 7157 (2000).
[6] G. S. Nolas, T. J. R. Weakley, J. L. Cohn, and R. Sharma, Phys. Rev. B **61**, 3845 (2000).
[7] E. Kaneshita and T. Nakayama, EPL **86**, 56004 (2009).
[8] K. Suekuni, M. A. Avila, K. Umeo, and T. Takabatake, Phys. Rev. B **75**, 195210 (2007).
[9] K. Suekuni, M. A. Avila, K. Umeo, H. Fukuoka, S. Yamanaka, T. Nakagawa, and T. Takabatake, Phys. Rev. B **77**, 235119 (2008).
[10] M. A. Avila, K. Suekuni, K. Umeo, H. Fukuoka, S. Yamanaka, and T. Takabatake, Appl. Phys. Lett. **92**, 041901 (2008).
[11] B. C. Sales, B. C. Chakoumakos, R. Jin, J. R. Thompson, and D. Mandrus, Phys. Rev. B **63**, 245113 (2001).
[12] B. C. Chakoumakos, B. C. Sales, and D. G. Mandrus, J. Alloys Compd. **322**, 127 (2001).
[13] B. C. Chakoumakos, B. C. Sales, D. G. Mandrus, and G. S. Nolas, J. Alloys Compd. **296**, 80 (2000).
[14] R. Baumbach, F. Bridges, L. Downward, D. Cao, P. Chesler, and B. Sales, Phys. Rev. B **71**, 024202 (2005).
[15] G. K. H. Madsen and G. Santi, Phys. Rev. B **72**, 220301(R) (2005).
[16] Y. Takasu, T. Hasegawa, N. Ogita, M. Udagawa, M. A. Avila, K. Suekuni, I. Ishii, T. Suzuki, and T. Takabatake, Phys. Rev. B **74**, 174303 (2006).
[17] M. A. Avila, K. Suekuni, K. Umeo, H. Fukuoka, S. Yamanaka, and T. Takabatake, Phys. Rev. B **74**, 125109 (2006).
[18] M. A. Avila, K. Suekuni, K. Umeo, and T. Takabatake, Physica B **383**, 124 (2006).
[19] M. Christensen, L. N. J. Overgaard, and B. B. Iversen, J. Am. Chem. Soc. **128**, 15657 (2006).
[20] J. Tang, R. Kumashiro, J. Ju, Z. Li, M. A. Avila, K. Suekuni, T. Takabatake, F. Guo, K. Kobayashi, and K. Tanigaki, Chem. Phys. Lett. **472**, 60 (2009).
[21] Y. Takasu, T. Hasegawa, N. Ogita, M. Udagawa, M. A. Avila, K. Suekuni, and T. Takabatake, Phys. Rev. Lett. **100**, 165503 (2008).
[22] T. Mori *et al.*, Phys. Rev. B **79**, 212301 (2009).
[23] K. Suekuni, Y. Takasu, T. Hasegawa, N. Ogita, M. Udagawa, M. A. Avila, and T. Takabatake, Phys. Rev. B **81**, 205207 (2010).
[24] W. Carrillo-Cabrera, S. Budnyk, Y. Prots, and Y. Grin, Z. Anorg. Allg. Chem. **630**, 2267 (2004).
[25] M. Christensen, A. B. Abrahamsen, N. B. Cristensen, F. Jurany, N. H. Andersen, K. Lefmann, J. Andreasson, C. R. H. Bahl, and B. B. Iversen, Nature Mater. **7**, 811 (2008).
[26] T. Hasegawa, Y. Takasu, N. Ogita, M. Udagawa, J.-I. Yamaura, Y. Nagao, and Z. Hiroi, Phys. Rev. B **77**, 064303 (2008).
[27] S. Tsutsui *et al.*, J. Phys. Soc. Jpn. **77**, 257 (2008), Suppl. A.
[28] S. Tsutsui *et al.*, J. Phys. Soc. Jpn. **77**, 033601 (2008).
[29] T. Hasegawa, Y. Takasu, T. Kondou, N. Ogita, M. Udagawa, T. Yamaguchi, T. Watanabe, Y. Nemoto, and T. Goto, J. Magn. Magn. Mater. **310**, 984 (2007).
[30] S. Kuroiwa, T. Hasegawa, T. Kondo, N. Ogita, M. Udagawa, and J. Akimitsu, Phys. Rev. B **78**, 184303 (2008).
[31] G. A. Slack, *CRC Handbook of Thermoelectrics* (CRC, Boca Raton, FL, 1995).